Neurobiology of Disease 45 (2012) 264–271

Contents lists available at SciVerse ScienceDirect

Neurobiology of Disease

journal homepage: www.elsevier.com/locate/ynbdi

Aberrant splicing and expression of the non muscle myosin heavy-chain gene *MYH14* in DM1 muscle tissues

F. Rinaldi [a], C. Terracciano [b], V. Pisani [b], R. Massa [b], E. Loro [c], L. Vergani [c], S. Di Girolamo [d], C. Angelini [c], G. Gourdon [e], G. Novelli [f,g], A. Botta [a,*]

[a] Dept. of Biopathology, Tor Vergata University of Rome, Rome, Italy
[b] Department of Neurosciences, Tor Vergata University of Rome, Rome, Italy
[c] Department of Neurosciences, University of Padua, Padua, Italy
[d] Department of Otolaryngology, Tor Vergata University of Rome, Rome, Italy
[e] INSERM, U781, Hôpital Necker-Enfants Malades, Université René Descartes Paris V, France
[f] San Peter Hospital, Fatebenefratelli, Rome, Italy
[g] National Agency for the Evaluation of Universities and Research, ANVUR, Rome, Italy

ARTICLE INFO

Article history:
Received 4 February 2011
Revised 25 July 2011
Accepted 3 August 2011
Available online 26 August 2011

Keywords:
Myotonic dystrophy
Spliceopathy
Non muscle myosins
Muscle pathology

ABSTRACT

Myotonic dystrophy type 1 (DM1) is a complex multisystemic disorder caused by an expansion of a CTG repeat located at the 3′ untranslated region (UTR) of DMPK on chromosome 19q13.3. Aberrant messenger RNA (mRNA) splicing of several genes has been reported to explain some of the symptoms of DM1 including insulin resistance, muscle wasting and myotonia. In this paper we analyzed the expression of the MYH14 mRNA and protein in the muscle of DM1 patients (n = 12) with different expansion lengths and normal subjects (n = 7). The MYH14 gene is located on chromosome 19q13.3 and encodes for one of the heavy chains of the so called class II "nonmuscle" myosins (NMHCII). MYH14 has two alternative spliced isoforms: the inserted isoform (NMHCII-C1) which includes 8 amino acids located in the globular head of the protein, not encoded by the non inserted isoform (NMHCII-C0). Results showed a splicing unbalance of the MYH14 gene in DM1 muscle, with a prevalent expression of the NMHCII-C0 isoform more marked in DM1 patients harboring large CTG expansions. Minigene assay indicated that levels of the MBNL1 protein positively regulates the inclusion of the MYH14 exon 6. Quantitative analysis of the MYH14 expression revealed a significant reduction in the DM1 muscle samples, both at mRNA and protein level. No differences were found between DM1 and controls in the skeletal muscle localization of MYH14, obtained through immunofluorescence analysis. In line with the thesis of an "RNA gain of function" hypothesis described for the CTG mutation, we conclude that the alterations of the MYH14 gene may contribute to the DM1 molecular pathogenesis.

1. Introduction

1.1. The myotonic dystrophy type 1 spliceopathy

Myotonic dystrophy type 1 (DM1; OMIM 160900) is the most prevalent form of muscular dystrophy in adults (Harper et al., 2001). This disorder is caused by the expansion of a CTG repeat in the 3′ untranslated region (UTR) of *DMPK* (*DMPK*; OMIM 605377), a gene encoding a protein kinase localized on chromosome 19q13.3 (Brook et al., 1992). The CTG repeats are polymorphic, healthy individuals that have 5–38 CTG repeats whereas individuals with DM1 have repeats in the hundreds to thousands (Zerylnick et al., 1995). The clinical aspects of the disease include myotonia, progressive muscle weakness, cataracts, insulin resistance and cardiac conduction defects (Harper et al., 2001). Three forms of DM1 are usually recognized: congenital DM1 (CDM), which is associated with generalized muscular hypotonia, talipes, and mental retardation; juvenile/adult DM1, phenotypically variable, with myotonia, muscle weakness, cardiac arrhythmias, male balding, hypogonadism, psychocognitive dysfunction, and glucose intolerance; and late adult/senile DM1, seen in middle-to-old-age and characterized by cataracts, baldness, and minimal or absent muscle involvement (Machuca-Tzili et al., 2005). The main pathogenic process at the basis of DM1 is a toxic RNA-gain of function effect of mutant *DMPK* transcripts which are retained in distinct ribonuclear foci within cells (Davis et al., 1997). A current model of the disease mechanism hypothesizes that CUG expanded tracts alter the function of at least two RNA-binding proteins involved in the alternative splicing process: the muscleblind-like 1 protein (MBNL1) and the CUG-binding protein 1 (CUGBP1) (Dansithong et al., 2005; Kuyumcu-Martinez et al., 2007; Miller et al., 2000). It has been

* Corresponding author at: Tor Vergata University of Rome, Dept. of Biopathology, Via Montpellier, 1, 00133 Rome, Italy. Fax: +39 6 20427313.
E-mail address: botta@med.uniroma2.it (A. Botta).
Available online on ScienceDirect (www.sciencedirect.com).

0969-9961/$ – see front matter © 2011 Elsevier Inc. All rights reserved.
doi:10.1016/j.nbd.2011.08.010

proposed that the MBNL1 loss of function, through a physical interaction with the CUG-repeats, and the CUGBP1 protein increased steady state level, due to a PKC mediated nuclear hyperphosphorylation, act synergistically in the splicing misregulation of a wide group of developmentally regulated genes (Kuyumcu-Martinez et al., 2007; Ranum, 2006). These include cardiac troponin T (*c-TNT*), insulin receptor (*IR*), muscle specific chloride channel (*CLCN-1*) and the dystrophin gene in skeletal muscle, the microtubule-associated tau, NMDA receptor 1 and amyloid precursor protein in the brain (Sergeant et al., 2001; Kalsotra et al., 2008; Osborne et al., 2009). In all cases the splicing regulation is disrupted, resulting in preferential expression of aberrant spliced isoforms not appropriate for a particular tissue or developmental stage. Among the symptoms of DM1, myotonia and insulin resistance are attributed to the disruption of the *CLCN-1* and *IR* alternative splicing, respectively (Charlet et al., 2002; Savkur et al., 2001). Moderate to severe hearing loss, usually sensorineural, has also been reported in DM1 patients (Wright et al., 1988) and the risk of developing serious hearing impairment is much greater for adult patients in all age brackets when compared to the general population (Wright et al., 1988). However, the cause of hearing problems in DM1 patients is not well defined.

1.2. Hearing loss and mammalian non muscle myosin heavy-chain gene MYH14

Hereditary hearing loss is caused, in 50% of cases, by single gene mutations, including myosins, connexins, transcription factors, potassium channels or other cellular components that play an important role in ear cells (Hilgert et al., 2009; Van Laer et al., 2003). Different members of the myosin superfamily are responsible for syndromic and non-syndromic hearing impairment transmitted as an autosomal dominant or recessive trait (Friedman et al., 1999). Mammalian non muscle myosin IIs (NM-IIs) are exameric proteins composed of two heavy chains and two pairs of light chains that self associate to form bipolar filaments that pull on actin filaments to produce the force that drives important cellular functions, such as cytokinesis, cell polarity and cell migration (Sellers, 2000). The term “nonmuscle myosin” was generally used to distinguish between the ubiquitous forms of myosin II and the muscle-specific isoforms. However, this term is misleading because these myosins are not only expressed in all types of non-muscle tissue but also have a significant role in the development and function of smooth and skeletal muscles (Morano et al., 2000; Takeda et al., 2000; Tullio et al., 1997). Three isoforms of the non-muscle myosin heavy chain (NMHC), II-A, II-B, II-C have been identified in vertebrates (Golomb et al., 2004; Katsuragawa et al., 1989), and are the product of three different genes: *MYH9*, *MYH10* and *MYH14*, respectively in humans (Leal et al., 2003; Simons et al., 1991). These myosins have a very high sequence homology both inter and intra species (Golomb et al., 2004) and although *MYH14* is still called “nonmuscle myosin” it is highly expressed in skeletal muscle like the other two nonmuscle myosins (Leal et al., 2003). The *MYH14* gene is located on chromosome 19q13.3, inside the DFN4A region associated with a non-syndromic autosomal dominant deafness (Donaudy et al., 2004; Pusch et al., 2004). The gene is composed of 41 exons and is transcribed as a main 7 kb mRNA which encodes for a potential polypeptide of 1995 aa and a calculated 228 kDa molecular weight (Leal et al., 2003). The identification of point mutations in large pedigrees linked to DFN4A clearly demonstrates the role of *MYH14* in causing autosomal dominant hearing loss and further confirms the crucial role of the myosin superfamily in auditive functions (Yang et al., 2005). Previous studies about this gene have identified at least two alternatively spliced isoforms across exon 6 which encode for the NMHC II-C0 and NMHC II-C1 isoforms differing by 8 aminoacids inserted into loop 1 in the globular head of the protein (Golomb et al., 2004). Interestingly, this insertion is near the ATP-binding region of NMHC II-C and increases both actin-activated MgATPase enzymatic activity and *in vitro* motility in translocating actin filaments of the inserted isoform (Kim et al., 2005). The purpose of the present study was to determine the expression profile of the *MYH14* gene at the mRNA and protein level in DM1 muscle tissues. To accomplish this, we analyzed 12 skeletal muscle biopsies from DM1 patients harboring different CTG expansions and 7 muscle biopsies from healthy controls. We found a splicing unbalance of the *MYH14* gene in DM1 muscle, with a prevalent expression of the $MYH14_{\Delta 6}$, not inserted isoform, mainly in patients with large DM1 mutations. An aberrant splicing regulation of the *Myh14* transcript has also been observed in the muscular tissue of the DMSXL mice models of DM1 with changes opposite to those in the muscle samples from patients. Quantitative analysis of the *MYH14* expression revealed a significant reduction in the DM1 muscle samples at both mRNA and protein levels, whereas no differences have been found in the skeletal muscle localization of the MYH14 protein between DM and control tissues. *In vitro* minigene assays demonstrated that MBNL1 directly regulates the splicing of *MYH14* pre-mRNA inducing the inclusion of exon 6. These findings indicate that the sequestration of MBNL1 in the CUG repeat expansion could lead to the expression of a *MYH14* shorter isoform which could play a role in the muscular and hearing impairment typical of DM1 patients.

2. Methods

2.1. Skeletal muscle biopsies and patients' clinical data

DM1 muscle samples (n = 12) and controls samples (n = 7) were diagnostic open biopsies from vastus lateralis provided by Telethon Biobank No. GTB07001. All muscle biopsies were frozen in melting isopentan immediately after surgery, and stored at −80 °C until used. Histological analysis of DM1 biopsies showed the typical pathology of the disease, including increased fiber size variation, atrophic fibers, pyknotic nuclear clamps, and marked prevalence of centrally located nuclei. DM1 patients were diagnosed at the Department of Neurology, University of Padua, Padua, Italy. The diagnosis of DM1 was based on clinical, electromyographic (high frequency repetitive discharges), ophthalmologic and cardiac investigations. In our cohort of patients, the degree of muscle impairment was assessed by using the Muscular Impairment Rating Scale (MIRS) (Mathieu et al., 2001). In addition to the MIRS we also assessed cognitive impairment, cataract, cardiac involvement, endocrine dysfunctions and motor impairment (Table 1).

Table 1
Clinical and molecular data of DM1 patients included in this study.

Patient code	MIRS	Cardiac involvement		Serum CK (IU/L)	Cataracts	$(CTG)_n$ in skeletal muscle
		CD	CM			
DM-1	1	None	None	115	ND	165
DM-2	2	None	ND	ND	Positive	275
DM-3	1	None	None	Normal	None	400
DM-4	2	None	None	ND	Positive	430
DM-5	1	None	ND	224	None	375
DM-6	2	RBB	None	419	Positive	360
DM-7	3	PM	FHK	Normal	ND	1350
DM-8	2	LAH-RBB	AI-MI-TI	169	Positive	1700
DM-9	2	AVB I	DC-MI-TI	307	Positive	1300
DM-10	1	None	ND	279	Positive	1250
DM-11	3	None	None	618	None	1300
DM-12	4	None	None	ND	ND	1900

ND: not done; CD: cardiac conduction; CM: cardiac morphology; AI: aortic insufficiency; AVB: atrio-ventricular block; DC: cardiac dilatation; FHK: focal hypokinesis; LAH: left anterior hemiblock; MI: mitral insufficiency; MP: mitral prolapse; PM: pace-maker; RBB: right branch block; TI: tricuspidal insufficiency. The normal values for CK is 0–170 U/L in females and 0–190 U/L in males.

2.2. Molecular analysis

Genomic DNA was extracted from skeletal muscle using a salting-out procedure (Miller et al., 1988). (CTG) repeat expansion sizes were determined by a combination of long-PCR and Southern blot analysis (Botta et al., 2006). Expanded fragments were sized by measuring the bands of major intensity which presumably corresponds to the more representative alleles. DM1 mutation in our muscle samples ranged from 150 up to 2000 (CTG)s (Tab.1).

2.3. QRT-PCR and splicing analysis

Total RNA was extracted from frozen muscle biopsies using TRI reagent (Molecular Research Center, Inc.). Three micrograms of total RNA was reverse transcribed according to the cDNA protocol of the High Capacity cDNA Archive kit (Applied Biosystem, Foster City, CA). The expression level of the *MYH14* gene was measured by Real-Time quantitative PCR (QRT-PCR) using the Hs00226855_m1 Assay-on-demand™ gene expression product, labeled with FAM-dye. The relative *MYH14* gene expression level in each cDNA sample has been obtained by a multiplex QRT-PCR reaction using a human β2-microglobulin (β2M) specific probe labeled with VIC™ MGB dye as internal control gene (TaqMan assay # Hu β2M 4326319 E). Each PCR reaction was performed in triplicate using the TaqMan™ gene expression Master Mix and the ABI PRISM 7000 Sequence Detection System (Applied Biosystem, Foster City, CA). A comparative threshold cycle (Ct) was used to determine gene expression. For each sample, *MYH14* Ct value was normalized with the internal control gene using the formula $\Delta Ct = Ct_{MYH14} - Ct_{\beta 2M}$. The distribution of ΔCt between DM1 samples and controls has been analyzed using a t-Student statistical analysis. The RT-PCR splicing assay to study the two alternative *MYH14* isoforms was performed according to a reported protocol using primers across the exon 6 gene region (Jana et al., 2006). Total PCR products, obtained within the linear range of amplification, were electrophoresed on 3% agarose gel. The $MYH14_{ex6}/MYH14_{\Delta 6}$ isoform ratio has been quantified by a QRT-PCR assay specific for the two different *MYH14* gene isoforms using the β2M transcript as internal control. Primers and probes across exon 6 and exons 5–7 have been designed on demand by Applied Biosystem on the basis of the *MYH14* gene transcript sequence (GenBank Accession number #NM_001077186.1). The *MYH14* isoform not including exon 6 has been detected with the following set of primers and probe: primer F 5′-TCTCCAAAGGGCAGGAAGGA-3′, probe 5′-CTCACCGGGGACACCC-3′ FAM labeled, primer R 5′-ATGGGGTTGGCCTGAAGCA-3′. The $MYH14_{ex6}$ isoform have been measured with primer F 5′-TCTCCAAAGGGCAGGAAGGA-3′, probe 5′-CCGTCAGCACCGTGTCT-3′ FAM labeled and primer R 5′-CCGCTCCAGCTCACCATA3′.

2.4. Construction of plasmids for MYH14 minigene assay

To construct the mini-gene that includes *MYH14* exons 5–7 (pcMYH2.5) the human genomic sequence of *MYH14* (RefSeqGene NG_011645.1) containing 32 bp of intron 4, exon 5–intron 5–exon 6–intron 6–exon 7 and of 90 bp of intron 7, was generated by PCR using the following primer sets: forward (MYHint4F 5′-AACCCCTTTGCTTCCCTT-3′) and reverse (MYHint7R 5′-ATCCACGTGTCTTTCCCCCT-3′). The approximately 2.5 kb PCR product was obtained and digested with BamHI and NotI, then subcloned in the pCR2.1 vector (Invitrogen Corp, Carlsbad, CA) and inserted into the pcDNA3.1(+) mammalian expression vector (Invitrogen Corp, Carlsbad, CA) digested with BamH1 and NotI enzymes. Standard recombinant DNA techniques were used to construct an expression plasmid for the MBNL1 isoforms 41 protein in the pEF1/-Myc-HisA vector (Invitrogen Corp, Carlsbad, CA) ($pEF1MBNL1_{41}$). All of the constructs were sequenced before use in the experiments. *In vitro* splicing constructs of human *MYH14* mini-genes (4.0 μg) were transfected into rabdomiosarcoma cells using LipofectAMINE2000 reagent (Invitrogen Corp, Carlsbad, CA) according to the manufacturer's protocol. Transfected cells were lysed in TRI reagent (Molecular Research Center, Inc.) 48 h after the addition of plasmids and the total cellular RNA was purified. First strand cDNA was synthesized in a 20-μl reaction volume using the High Capacity cDNA Archive kit protocol (Applied Biosystem, Foster City, CA). PCR amplification analysis of the plasmid-derived cDNAs was performed using the primer set and the MYHint4F and pcDNA3.1/BGH reverse priming site. The reaction products were resolved by 2.5 agarose gel electrophoresis and quantitative analysis of the amplified products was carried out using a fluorimager 595 (Amersham Biosciences, Buckinghamshire, UK). The ratio of exon 6 inclusion was quantified and expressed as percentages of inclusion relative to the total intensities. Data are shown as the mean + SD of three independent experiments.

2.5. Transgenic mice

The transgenic mice used in this study carry 45 kb of human genomic DNA cloned from a DM1 patient as described by Gomes-Pereira et al. (2007). Animals were bred onto a mixed background (C57BL6/129/OLA/FVB). Transgenic status and CTG molecular sizing was assayed by Tail PCR using reported protocols (Seznec et al., 2000). Total RNA has been extracted from proximal (vastus lateralis—VL) and distal (gastrocnemius—GM) skeletal muscles, brain and heart of two mice homozygous for hDMPK alleles (700/1230) at 6 months of age and two age-matched non-transgenic littermates. The ratio of the inserted and non inserted *Myh14* transcripts has been determined by RT-PCR according (Golomb et al., 2004). All experiments were performed in accordance with the Directive 2010/63/EU.

2.6. Western blotting

Ten micrometer muscle sections were collected from frozen biopsy specimens and lysed in a buffer containing 50 mM Tris pH 7.5, 150 mM NaCl, 10 mM $MgCl_2$, 0.5 mM DTT, 1 mM EDTA, 10% glycerol, 2% SDS, 1% Triton X-100, Protease Inhibitor Cocktail (Sigma Aldrich) and Phosphatase Inhibitor Cocktail 1 and 2 (Sigma Aldrich). Protein amount was measured by the BCA method (Pierce) and 30 μg of each extract was run in a 4–12% T30C4 SDS-PAGE. Proteins were then blotted into a nitrocellulose membrane, probed with specific NMHCII-C 1:600 (Golomb et al., 2004) and actin 1:5000 (Santa Cruz BT) antibodies. After incubation with secondary HRP-conjugated antibodies, recognized bands were visualized by chemiluminescence (GE HealthCare). Integrated optical density of each band was calculated with commercial software and normalized compared to the actin levels.

2.7. Immunofluorescence analysis

Longitudinal and transverse muscle cryostat sections (8 μm) of normal subjects and DM1 patients were thaw-mounted on to glass slides pretreated with 3% EDTA to prevent contracture artifacts, and processed for indirect immunofluorescence (IF). After fixation in acetone for 10 min at 4 °C, sections were incubated for 60 min with the anti-NMHCIIc Ab, diluted 1:100 (kindly provided by Prof. R. Adelstein), rinsed in PBS and incubated for 1 h with a TRITC-conjugated goat anti-rabbit Ab (Sigma, 1:100). Negative control sections were incubated with non-immune serum instead of primary Ab. In order to evaluate localization of NMHC II-C in relation to sarcomeric components, double-labeling experiments were conducted combining the anti-NMHC II-C with an anti-slow Myosin Heavy Chain (sMHC) monoclonal Ab (Novocastra, Newcastle upon Tyne, UK, 1:10).

3. Results

3.1. Aberrant splicing of the MYH14 transcript in muscle tissue from DM1 patients and DMSXL transgenic mice

The gene encoding NMHC II-C undergoes alternative splicing to generate several isoforms. One of these isoforms, named NMHC II-C1, contains the alternatively spliced exon 6 that encodes for 8 amino acids close to the ATP binding region in loop 1 of the protein (Golomb et al., 2004). The NMHC II-C1 protein is expressed in a variety of tissues and shows an increased actin-activated MgATPase activity and *in vitro* motility compared with the non inserted isoform (NMHC II-C0). To test whether the *MYH14* gene expression is altered in DM1 patients, we investigated the expression and the splicing pattern of this gene in human skeletal muscle biopsies of 12 DM1 patients and 7 control subjects.

Total amount of *MYH14* transcript was determined in DM1 muscles and in controls using a QRT-PCR approach with a *MYH14*-specific TaqMan assay. For each sample, *MYH14* expression was normalized with the gene *B2-microglobulin* (*B2-M*) as an endogenous control. Results shown in Fig. 1 indicate the down regulation of the *MYH14* transcript in the DM1 skeletal muscle compared to normal samples. In DM1 patients, the reduction of the *MYH14* mRNA ranged from 19% to 88%, with no correlation with the CTG expansion grade (median control values has been set as 100%).

We also investigated the expression of the alternative spliced isoforms encoding for the NMHC II-C0 and NMHC II-C1 proteins in muscle biopsies using conventional RT-PCR with primers flanking *MYH14* exon 6. Fig. 2A shows the distribution of the $MYH14_{ex6}$ (NMHCII-C1) and $MYH14_{\Delta 6}$ (NMHCII-C0) isoforms in our set of muscle biopsies. The figure shows that, although the inserted mRNA is predominant in control samples, DM1 muscles express an increasing amount of the non inserted isoforms proportionate to the CTG expansion grade. Quantification of the two *MYH14* transcripts was calculated by QRT-PCR analysis using two different TaqMan probes specific for the $MYH14_{ex6}$ and $MYH14_{\Delta 6}$ isoforms respectively and the *B2-M* transcript as a control for the normalization of samples. The diagram in Fig. 2B indicates that the median value of the $MYH14_{\Delta 6}/MYH14_{ex6}$ isoform ratio is 0.24 for the controls and 0.72 for the DM1 patients, with higher levels in DM1 patients harboring more than 1000 CTG repetitions. Statistical analysis of these values indicates that the difference between DM1 and controls is significant with a P value < 0.03.

Transgenic mice offer an important model of what occurs in human patients and are powerful tools with which we can understand the pathogenesis of DM1. To further confirm the aberrant splicing of the *MYH14* gene in DM1 we studied the expression of the mouse *Myh14* orthologue gene (GenBank accession number #BAB26815) in the well-characterized DMSXL mouse model (Gomes-Pereira et al., 2007). These mice are homozygous for the human DM1 mutation, carrying 700 CTG on one allele and more than 1000 on the other. They displayed a severe disease phenotype with very high mortality, growth retardation from birth and marked splicing abnormalities in the central nervous system and muscle (Gomes-Pereira et al., 2007). The mouse *Myh14* shows 90% identity with the human homologue gene and maintains the two alternatively spliced isoforms expressed in humans (GenBank accession numbers #AY205605 and #AY363100) encoding for proteins which contain the characteristic domains of a myosin II heavy chain. The corresponding cDNAs encode a gene product of 2000 aa for the inserted isoforms and 1992 aa for the non inserted one.

We used RT-PCR analysis to determine the ratio of the inserted and non inserted *Myh14* transcripts in proximal (vastus lateralis-VL) and distal (gastrocnemius-GM) skeletal muscle, brain and heart tissues from two mice homozygous for hDMPK locus (700/1230) at 6 months of age and from two age-matched non-transgenic littermates. As reported in literature (Golomb et al., 2004), adult mouse skeletal muscle and heart express very low amounts of the *Myh14* inserted message in contrast to what is observed in the human tissues. In brain tissue there is approximately equal amounts of both mRNAs. In DMSXL mice we observed an aberrant splicing of the *Myh14* gene in both VL and GM muscles with an increased expression of the inserted message (more marked in the distal muscle) compared to the wild type tissues. However, the splicing alterations found in DMSXL mice and DM1 patients are opposite, which could be explained by the different *MYH14* isoform expression in the wild type tissues of mice and humans. No significant differences of the *Myh14* expression profile have been found in the heart and brain between DMSXL and control mice (Fig. 3).

To determine the *cis*-acting elements responsible for the aberrant splicing of the *MYH14* gene, we searched the binding sequences for the MBNL1 and CUGBP1 splicing factors in *MYH14* exon 6 and its 180 bp flanking intron sequences. We found 3 repeats of the specific sequence for MBNL1-binding, YGCU(U/G)Y: one located 38 nt upstream and the other two at 28 and 151 nt downstream of the exonic region. Moreover, 6 YCGY repeats (two located in intron 5 and 4 in intron 6 respectively) and several YCG or CGY motifs have been detected. *Cis*-elements responsible for the CUGBP1 binding (TGTTTGTTTGT or TGTGTGTGTGT) were not observed in *MYH14* exon 6 and in its flanking intronic sequences. MBNL1 could therefore regulate the alternative splicing of the *MYH14* gene by binding specific motifs in the intronic region flanking exon 6 leading to the mis-splicing observed in DM1 muscle.

To verify this hypothesis, we constructed a minigene including the human sequence of *MYH14* containing 32 bp of intron 4, exon 5–intron 5–exon 6–intron 6–exon 7 and 90 bp of intron 7 cloned into a

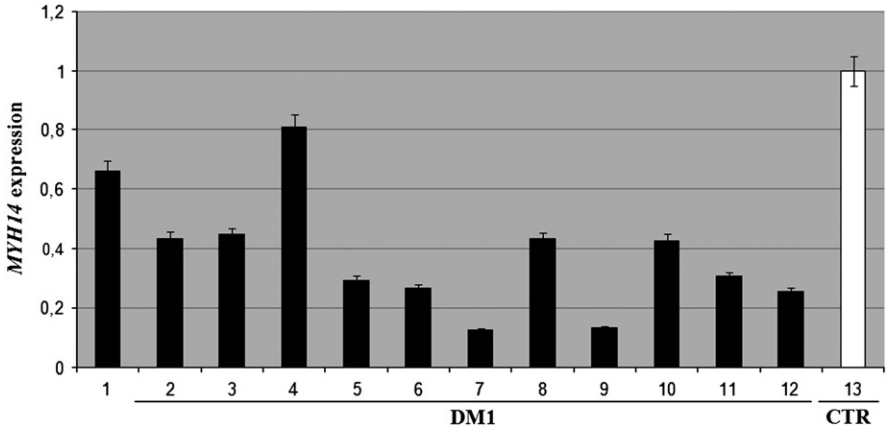

Fig. 1. Total expression level of the *MYH14* gene in DM1 and control samples. The relative *MYH14* gene expression in each cDNA sample has been obtained by a multiplex QRT-PCR reaction using the TaqMan technology with the *B2-microglobulin* gene as internal control gene. Each reaction has been conducted in triplicate and control sample, set as 1, indicates the median value of controls ($n = 7$).

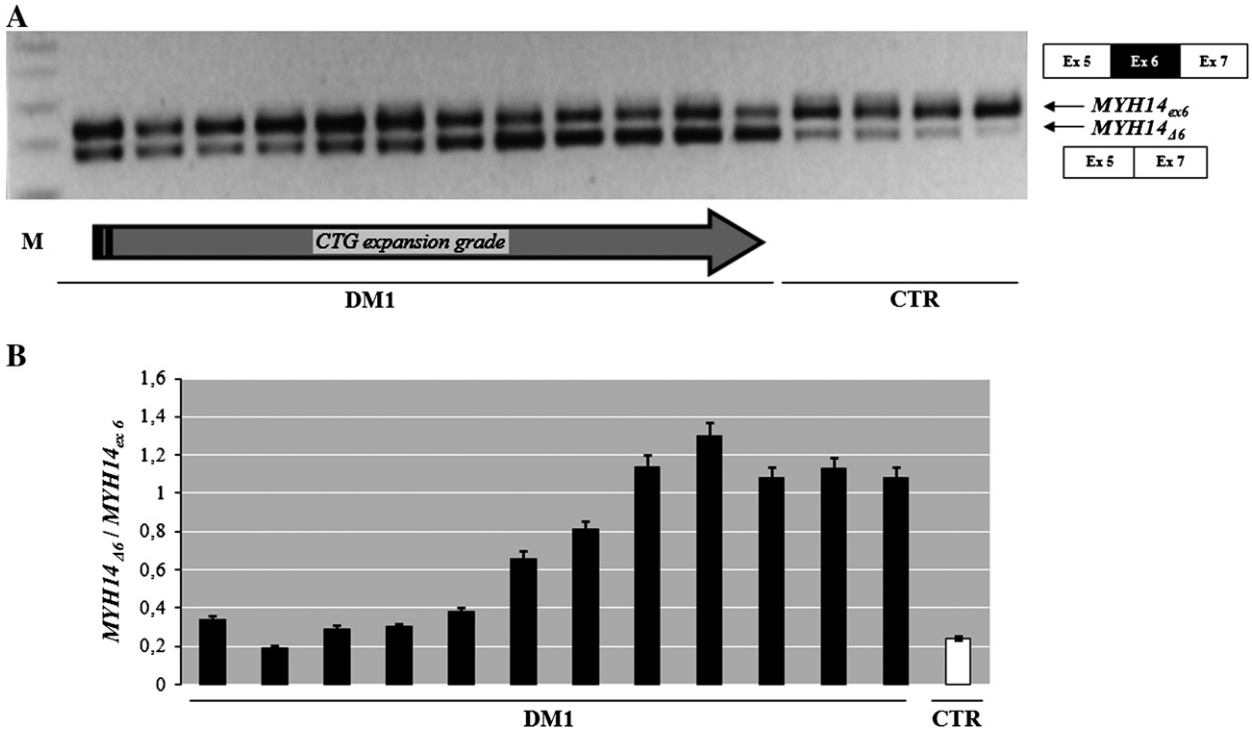

Fig. 2. A) RT-PCR analysis of the $MYH14_{\Delta 6}$ and $MYH14_{ex6}$ isoforms in DM1 and control muscles. DM1 samples have been loaded according to the CTG expansion grade. A schematic representation of the human *MYH14* analyzed exons is also reported. B) Quantitative QRT-PCR assays to measure the expression of the different *MYH14* gene isoforms. The relative *MYH14* gene expression in each cDNA sample has been obtained by a multiplex QRT-PCR reaction using TaqMan probes recognizing the *MYH14Δ6* and the *MYH14ex6* transcripts and the *B2-microglobulin* gene as internal control.

pcDNA3.1 vector (pcMYH2.5) (Fig. 4A). We transfected the pcMYH2.5 plasmid into human rabdomiosarcoma cells. RT-PCR, using a combination of plasmid and *MYH14*-specific primers (see Methods), showed that the minigene expressed mRNAs both with the inclusion and the exclusion of *MYH14* exon 6, with a prevalence of the shorter isoform (Fig. 4B). The pcMYH2.5 construct was therefore transiently co-transfected with the expression vector for the MBNL1 isoform 41 ($pEF1MBNL1_{41}$) using a plasmid expressing the EGFP protein (pEGFP) to monitor the transfection efficiency. Total RNA was collected after 48 h and RT-PCR was performed using a combination of *MYH14* and plasmid-specific primers to detect RNA processing of *MYH14* gene in transfected rabdomiosarcoma cells. The expression of the MBNL1 protein promoted the inclusion of *MYH14* exon 6 compared with cells transfected with the minigene alone (Fig. 4B). The ratios of exon 6 inclusion (*MYH14*exon6/*MYH14*total) was 35%±2% using the mini-gene alone and 86%±4% when the MBNL1 protein was co-expressed (Fig. 4C). Taken together, these findings suggest that the MBNL1 protein could specifically promote the inclusion of the *MYH14* exon 6 acting on specific *cis*-elements in the pcMYH2.5 mini-gene genomic sequence.

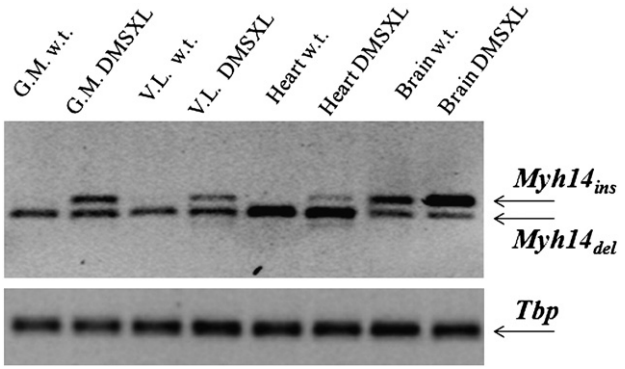

Fig. 3. RT-PCR analysis of the $Myh14_{ins}$ $Myh14_{del}$ isoforms of the *Myh14* mouse orthologue in different tissues of wild type and DMSXL mice. Tissues analyzed are: proximal (vastus lateralis—VL) and distal (gastrocnemius—GM) skeletal muscles, brain and heart.

3.2. The NMHC-II protein is down-regulated in DM1 muscle but retains its subcellular localization

In order to study the expression and the localization of the NMHC II-C protein in muscle from DM1 patients and controls, we used an antibody raised to the mouse C-terminal sequence of the protein (kindly provided by Prof. R. Adelstein). The specificity of this antibody among the three NMHCs proteins has been demonstrated by immunoblot and immunoprecipitation analyses (Golomb et al., 2004). Protein extracts from 8 DM1 skeletal muscle biopsies and 7 controls were tested by Western blot assay using actin for normalization of the samples. Fig. 5A shows immunoblotting incubated with an antibody to NMHC II-C that recognizes a 200 kDa signal expressed in both DM1 and control tissues. Diagram 5B quantifies the integrated optical density of NMHC II-C normalized with actin. Interestingly, in DM1 patients there is a marked reduction of the NMHC II-C level with NMHCII-C/actin median value of 0.24 in DM1 samples and 0.42 in controls. Experiments were repeated three times and the Student's t test demonstrated that the observed difference is statistically significant with a P value <0.03.

To precisely localize the NMHC II-C protein in the muscle tissues from DM1 patients and controls, we performed immunofluorescence analysis on longitudinal muscle section ($n=3$ DM1 samples and $n=3$ control samples). For this study, DM1 patients harboring more than 1000 CTG repetitions were chosen. Immunofluorescence showed that the NMHC II-C protein is highly expressed in human skeletal muscle, with no apparent differences between muscle fiber types. In longitudinal sections stained for NMHC II-C, a neat signal with a

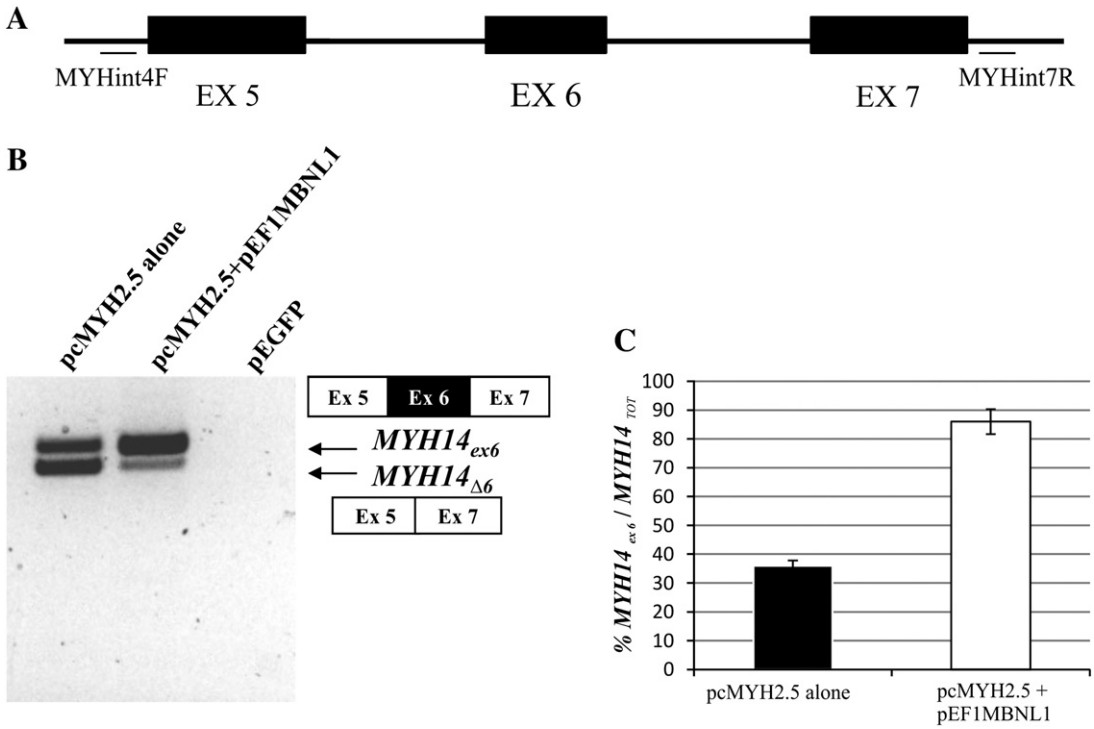

Fig. 4. A) Schematic representation of the 2.5 kb genomic sequence from *MYH14* containing exon 5–intron 5–exon 6–intron 6–exon 7. Positions of the MYHint4F and MYHint7R are also indicated. B) RT-PCR analysis using primers MYHint4F and pcDNA3.1/BGH reverse of RNA extracted from rabdomiosarcoma cells transfected with: pcMYH2.5 alone (lane 1), pcMYH2.5 and pEF1MBNL1$_{41}$ (lane 2) and pEGFP alone (lane 3). C) Percentages of *MYH14* exon 6 inclusion relative to the total *MYH14* transcript (MYH14 ex6/total MYH14).

regular transverse banding pattern, spanning throughout the fiber width, was observed (Fig. 6). The transverse elements were consistently 0.8–1 μm wide (Fig. 6) roughly corresponding to the sarcomeric I band width. Indeed, dual immunolabeling using a combination of antibodies against NMHC II-C and sMHC showed a complete separation of the two fluorescent patterns, with that of NMHC II-C occupying the space between the sMHC, (A bands) (Fig. 6C). These findings suggest that NMHC II-C has a subcellular location within or in proximity of the I band (Fig. 6). This pattern did not differ between DM1 and normal muscles indicating that the aberrant *MYH14* splicing does not affect the NMHC II-C muscular distribution, however the intensity of NMHC II-C fluorescent signal seemed lower in DM1 samples than in normal controls according to Western blot analysis (Figs. 6A and B).

4. Discussion

The present study reports the expression profile of the *MYH14* gene at the mRNA and protein level in DM1 muscle tissue compared to controls. DM1 is a multisystemic disorder that affects the eye, cardiovascular apparatus, endocrine apparatus, gall bladder, testicular system, in addition to the muscle apparatus (Harper et al., 2001). Moderate to severe hearing loss has also been identified in some patients with both a peripheral and central level involvement of the

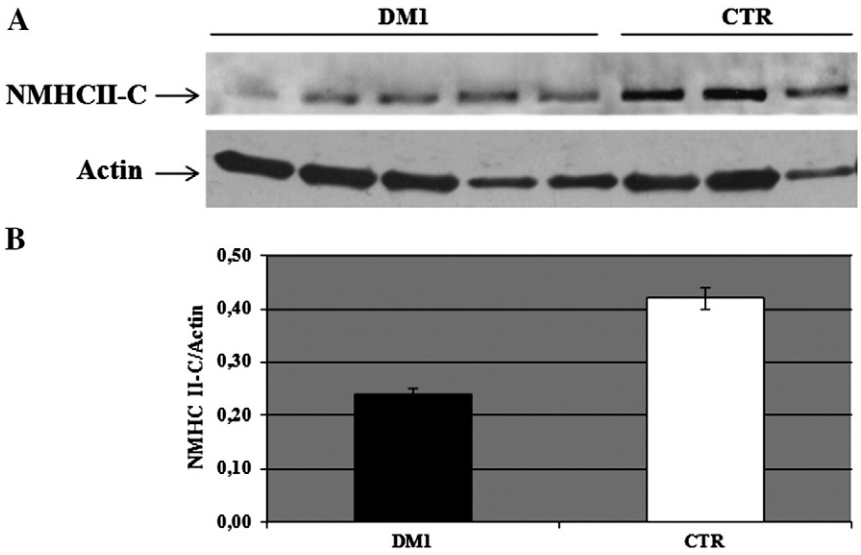

Fig. 5. A) Western blot analysis on muscle lisates from DM1 and controls using an NMHCII-C antibody which recognizes a 200 kDa band. The β-actin protein has been used for the normalization of samples. B) Bar chart reporting the integrated optical density, normalized with β-actin, of the NMHC II-C protein levels in DM1 and in controls muscle samples. The experiment was repeated three times and data are expressed as mean ± standard error of the mean.

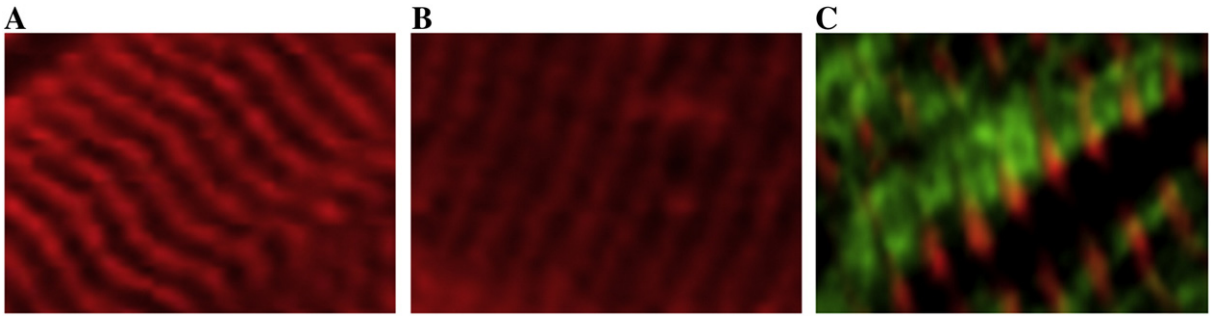

Fig. 6. (A and B) NMHC II-C single label immunofluorescence (IF) in human skeletal muscle shows intracellular distribution with a transverse banding pattern. No difference in the distribution was found between normal controls (A) and DM1 patients (B) (longitudinal section, ×40). (C) Double label IF with NMHC II-C (red) and MHC-slow (green) antibodies shows an alternate localization of NMHC II-C and of the A band marker MHC-slow (original magnification ×40).

auditory system (Huygen et al., 1994; Wright et al., 1988). Recently our group also reported that cochlear impairment in DM1 is present, even in patients without evidence of hearing loss as determined by a standard audiometric analysis (Pisani et al., in press). Misregulated alternative splicing in DM1 has been demonstrated for several mRNAs which contribute to the muscle, endocrine and cognitive symptoms of patients. The cause of the progressive muscle wasting and other extramuscular manifestations including hearing loss, however, has yet to be completely explained. The high expression of NMHC II-C in skeletal muscle, together with the alternative splicing process of the corresponding mRNA and its involvement in deafness, led us to suggest a possible role of this gene in the molecular pathogenesis of muscle disease and hearing impairment typical of DM1 patients. Our findings show that the aberrant splicing of the *MYH14* gene and the down-regulation of the transcript and protein levels in muscle tissues from DM1 patients seem to confirm this hypothesis. The 8 aminoacid-long C1 insert, encoded by *MYH14* exon 6, is located into loop 1 of the NMHC protein, in a region critical for binding with actin (Kim et al., 2005). The predominant expression of the $Myh14_{\Delta 6}$ isoforms observed in DM1 muscles predicts the production of an increasing level of the NMHC II-C0 protein, whose activity and *in vitro* motility is lower than the inserted isoform, which is predominantly found in controls. Interestingly, the degree of splicing unbalance seems to correlate with the length of CTG repetition and this is in accordance to what has been already observed by our group for other genes (Botta et al., 2008). Taken together these results strengthen the possibility that the CUG expansion could interfere with the processing of the *MYH14* pre-mRNA in a length-dependent manner. We also observed that the *Myh14* mouse homologue gene undergoes a splicing alteration in the muscle tissue of transgenic DMSXL mice older than 6 months of age, compared to age-matched healthy littermates. However, the *MYH14* splicing patterns observed in DMSXL mice and DM1 patients are opposite. These differences between the two species may arise, among other possibilities, from differences in the muscle-specific distribution of *MYH14* mRNA isoforms between mice and humans: non inserted *Myh14* isoform predominates in mouse skeletal muscle whereas $MYH14_{ex6}$ is the major isoform in the human tissue. We then searched specific sequences for splicing regulation around *MYH14* exon 6 and found that there are 3 "YGCU(U/G)Y" motifs and 6 "YGCY" sequences in intron 5 and 6 of the gene. These motifs have been shown to directly interact with the MBNL1 protein and mediate the *c-TNT* and *IR* gene alternative splicing (Grammatikakis et al., 2010). MBNL1 could therefore regulate the alternative splicing of the *MYH14* gene leading to the missplicing observed in DM1 muscle. This hypothesis has been confirmed by a minigene assay showing that the overexpression of MBNL1 protein promotes the inclusion of the *MYH14* exon 6 acting on specific *cis*-elements in the *MYH14* mini-gene genomic sequence.

In this study, we also observed decreased *MYH14* mRNA and protein levels in muscle of DM1 patients. The expression of the NMHC II-C inserted isoform is therefore also lowered by the concomitant reduction of the *MYH14* transcript and protein product in DM1 tissues. We suggest that this deleterious effect could be mediated by the CUG-containing RNA expansions through a transcriptional mechanism driven by direct binding of basic transcription factors (TFs), by epigenetic modifications of the DM1 locus (Ebralidze et al., 2004; López Castel et al., 2011), or may be due to a reduced stability of the *MYH14* transcript in DM1 tissues. Although there is considerable information concerning the role of myosins in cytokinesis (Krendel & Mooseker, 2005; Sellers, 2000), little is known about the individual role of each of the NMHC isoforms in this process. Studies conducted in Hela and A549 cells show a defect during cytokinesis, cell spreading and adhesion when the motor activity of NMHC proteins is inhibited (Jana et al., 2006). On the other hand, functional redundancy of the nonmuscle myosin II isoforms in cytokinesis has been reported and all three NMHC II isoforms are capable of rescuing multinucleation and cell dividing defects. The NMHC II-C protein localizes to the intercellular bridge where it is necessary, but not sufficient, for cytokinesis in the dividing process. In mouse and humans, NMHC II-A and NMHC II-B have been described to localize to the Z-lines and intercalated disks in cardiac muscle cells and near to the Z-lines in skeletal muscles (Takeda et al., 2000). NMHC II-A and II-B seem to have roles in the formation of myofibrils and to both be components of the complex cytoskeletal network required for maintaining the structural integrity of skeletal muscle. Thus far, no immunofluorescence study has been able to determine the muscular localization of the NMHC II-C protein in humans. In the last part of this study we showed that the NMHC II-C protein is strongly expressed in the muscle tissue and more specifically localizes in proximity of the sarcomeric I band, with a pattern of distribution very similar to that showed for NMHC II-A and II-B (Kee et al., 2009). No significant differences in the localization of the protein have been observed between DM1 and control samples, indicating that the aberrant splicing of the *MYH14* gene does not affect the distribution of the NMHC II-C protein. Further studies should clarify the precise subcellular localization and function of NMHC II-C in skeletal muscle fibers and cultures. In particular, it remains to be determined whether NMHC II-C is part of the sarcomeric apparatus or it concurs with other known proteins to form a perimyofibrillar cytoskeletal lattice.

In conclusion, we report for the first time the splicing alteration of the *MYH14* gene in DM1 muscle where reduced *MYH14* mRNA and protein levels have also been observed. These changes might disrupt the putative function of NMHC II-C in the cytoskeletal machinery and contribute to the pathogenesis of the typical DM1 histopathological features, such as central nuclei, ring fibers, sarcoplasmic masses. In parallel, similar alterations in NMHC II-C in the cochlea of DM1

patients may reduce hair cell contractility, contributing to the hearing impairment phenotype observed in this disease.

Acknowledgments

We wish to thank Robert Adelstein for antibodies against NMHC IIC. We also thank Dr. Lucia Rocchi and Dr. Giulia Rossi for their help in the construction of pcMYH2.5 minigene and pEF1MBNL1 vector. This work was supported by AFM grant #13360. Muscle samples were provided by Telethon Biobank No. GTB07001.

Competing interests: Authors declare that they do not have any competing interests.

References

Botta, A., Bonifazi, E., Vallo, L., Gennarelli, M., Garrè, C., Salehi, L., et al., 2006. Italian guidelines for molecular analysis in myotonic dystrophies. Acta Myol. 25 (1), 23–33.

Botta, A., Rinaldi, F., Catalli, C., Vergani, L., Bonifazi, E., Romeo, V., et al., 2008. The CTG repeat expansion size correlates with the splicing defects observed in muscles from myotonic dystrophy type 1 patients. J. Med. Genet. 45 (10), 639–646.

Brook, J.D., McCurrach, M.E., Harley, H.G., Buckler, A.J., Church, D., Aburatani, H., et al., 1992. Molecular basis of myotonic dystrophy: expansion of a trinucleotide (CTG) repeat at the 3′ end of a transcript encoding a protein kinase family member. Cell 69 (2), 385.

Charlet, B.N., Savkur, R.S., Singh, G., Philips, A.V., Grice, E.A., Cooper, T.A., 2002. Loss of the muscle-specific chloride channel in type 1 myotonic dystrophy due to misregulated alternative splicing. Mol. Cell 10, 45–53.

Dansithong, W., Paul, S., Comai, L., Reddy, S., 2005. MBNL1 is the primary determinant of focus formation and aberrant insulin receptor splicing in DM1. J. Biol. Chem. 280, 5773–5780.

Davis, B.M., McCurrach, M.E., Taneja, K.L., Singer, R.H., Housman, D.E., 1997. Expansion of a CUG trinucleotide repeat in the 3′ untranslated region of myotonic dystrophy protein kinase transcripts results in nuclear retention of transcripts. Proc. Natl. Acad. Sci. U.S.A. 94, 7388–7393.

Donaudy, F., Snoeckx, R., Pfister, M., Zenner, H.P., Blin, N., Di Stazio, M., et al., 2004. Nonmuscle myosin heavy-chain gene MYH14 is expressed in cochlea and mutated in patients affected by autosomal dominant hearing impairment (DFNA4). Am. J. Hum. Genet. 74 (4), 770–776.

Ebralidze, A., Wang, Y., Petkova, V., Ebralidse, K., Junghans, R.P., 2004. RNA leaching of transcription factors disrupts transcription in myotonic dystrophy. Science 303 (5656), 383–387.

Friedman, T.B., Sellers, J.R., Avraham, K.B., 1999. Unconventional myosins and the genetics of hearing loss. Am. J. Med. Genet. 89 (3), 147–157.

Golomb, E., Ma, X., Jana, S.S., Preston, Y.A., Kawamoto, S., Shoham, N.G., et al., 2004. Identification and characterization of nonmuscle myosin II-C, a new member of the myosin II family. J. Biol. Chem. 279 (4), 2800–2808.

Gomes-Pereira, M., Foiry, L., Nicole, A., Huguet, A., Junien, C., Munnich, A., et al., 2007. CTG trinucleotide repeat "big jumps": large expansions, small mice. PLoS Genet. 3 (4), e52.

Grammatikakis, I., Goo, Y.H., Echeverria, G.V., Cooper, T.A., 2010. Identification of MBNL1 and MBNL3 domains required for splicing activation and repression. Nucleic Acids Res.

Harper, P.S., Brook, J.D., Newman, E., 2001. Myotonic Dystrophy. W. B. Saunders, London, New York.

Hilgert, N., Smith, R.J., Van Camp, G., 2009. Forty-six genes causing nonsyndromic hearing impairment: which ones should be analyzed in DNA diagnostics? Mutat. Res. 681, 189–196.

Huygen, P.L., Verhagen, W.I., Noten, J.F., 1994. Auditory abnormalities, including 'precocious presbyacusis', in myotonic dystrophy. Audiology 33 (2), 73–84.

Jana, S.S., Kawamoto, S., Adelstein, R.S., 2006. A specific isoform of nonmuscle myosin II-C is required for cytokinesis in a tumor cell line. J. Biol. Chem. 281 (34), 24662–24670 Aug 25.

Kalsotra, A., Xiao, X., Ward, A.J., Castle, J.C., Johnson, J.M., Burge, C.B., et al., 2008. A postnatal switch of CELF and MBNL proteins reprograms alternative splicing in the developing heart. Proc. Natl Acad. Sci. U.S.A. 105 (51), 20333–20338.

Katsuragawa, Y., Yanagisawa, M., Inoue, A., Masaki, T., 1989. Two distinct nonmuscle myosin-heavy-chain mRNAs are differentially expressed in various chicken tissues. Identification of a novel gene family of vertebrate non-sarcomeric myosin heavy chains. Eur. J. Biochem. 184 (3), 611–616.

Kee, A.J., Gunning, P.W., Hardeman, E.C., 2009. Diverse roles of the actin cytoskeleton in striated muscle. J. Muscle Res. Cell Motil. 30 (5–6), 187–197.

Kim, K.Y., Kovács, M., Kawamoto, S., Sellers, J.R., Adelstein, R.S., 2005. Disease-associated mutations and alternative splicing alter the enzymatic and motile activity of nonmuscle myosins II-B and II-C. J. Biol. Chem. 280 (24), 22769–22775.

Krendel, M., Mooseker, M.S., 2005. Myosins: tails (and heads) of functional diversity. Physiology (Bethesda) 20, 239–251.

Kuyumcu-Martinez, N.M., Wang, G.S., Cooper, T.A., 2007. Increased steady-state levels of CUGBP1 in myotonic dystrophy 1 are due to PKC-mediated hyperphosphorylation. Mol. Cell 28, 68–78.

Leal, A., Endele, S., Stengel, C., Huehne, K., Loetterle, J., Barrantes, R., Winterpacht, A., Rautenstrauss, B., 2003. A novel myosin heavy chain gene in human chromosome 19q13.3. Gene 312, 165–171.

López Castel, A., Nakamori, M., Tomé, S., Chitayat, D., Gourdon, G., Thornton, C.A., 2011. Expanded CTG repeat demarcates a boundary for abnormal CpG methylation in myotonic dystrophy patient tissues. Hum. Mol. Genet. 20 (1), 1–15.

Machuca-Tzili, L., Brook, D., Hilton-Jones, D., 2005. Clinical and molecular aspects of the myotonic dystrophies: a review. Muscle Nerve 32 (1), 1–18.

Mathieu, J., Boivin, H., Meunier, D., Gaudreault, M., Bégin, P., 2001. Assessment of a disease-specific muscular impairment rating scale in myotonic dystrophy. Neurology 56, 336–340.

Miller, S.A., Dykes, D.D., Polesky, H.F., 1988. A simple salting out procedure for extracting DNA from human nucleated cells. Nucleic Acids Res. 16 (3), 1215.

Miller, J.W., Urbinati, C.R., Teng-Umnuay, P., Stenberg, M.G., Byrne, B.J., Thornton, C.A., Swanson, M.S., 2000. Recruitment of human muscleblind proteins to (CUG)(n) expansions associated with myotonic dystrophy. EMBO J. 19, 4439–4448.

Morano, I., Chai, G.X., Baltas, L.G., Lamounier-Zepter, V., Lutsch, G., Kott, M., et al., 2000. Smooth-muscle contraction without smooth-muscle myosin. Nat. Cell Biol. 2 (6), 371–375.

Osborne, R.J., Lin, X., Welle, S., Sobczak, K., O'Rourke, J.R., Swanson, M.S., Thornton, C.A., 2009. Transcriptional and post-transcriptional impact of toxic RNA in myotonic dystrophy. Hum. Mol. Genet. 18 (8), 1471–1481.

Pisani, V., Tirabasso, A., Mazzone, S., Terracciano, C., Botta, A., Novelli, G., Bernardi, G., Massa, R., Di Girolamo, S., 2011. Early subclinical cochlear dysfunction in myotonic dystrophy type 1. Eur. J. Neurol. Jul 21. [Epub ahead of print].

Pusch, C.M., Meyer, B., Kupka, S., Smith, R.J., Lalwani, A.K., Zenner, H.P., et al., 2004. Refinement of the DFNA4 locus to a 1.44 Mb region in 19q13.33. J. Mol. Med. 82 (6), 398–402.

Ranum, L.P., Cooper, T.A., 2006. RNA-mediated neuromuscular disorders. Annu. Rev. Neurosci. 29, 259–277.

Savkur, R.S., Philips, A.V., Cooper, T.A., 2001. Aberrant regulation of insulin receptor alternative splicing is associated with insulin resistance in myotonic dystrophy. Nat. Genet. 29, 40–47.

Sellers, J.R., 2000. Myosins: a diverse superfamily. Biochim. Biophys. Acta 1496 (1), 3–22.

Sergeant, N., Sablonnière, B., Schraen-Maschke, S., Ghestem, A., Maurage, C.A., Wattez, A., et al., 2001. Dysregulation of human brain microtubule-associated tau mRNA maturation in myotonic dystrophy type 1. Hum. Mol. Genet. 10 (19), 2143–2155.

Seznec, H., Lia-Baldini, A.S., Duros, C., Fouquet, C., Lacroix, C., Hofmann-Radvanyi, H., Junien, C., Gourdon, G., 2000. Transgenic mice carrying large human genomic sequences with expanded CTG repeat mimic closely the DM CTG repeat intergenerational and somatic instability. Hum. Mol. Genet. 9 (8), 1185–1194.

Simons, M., Wang, M., McBride, O.W., Kawamoto, S., Yamakawa, K., Gdula, D., Adelstein, R.S., Weir, L., 1991. Human nonmuscle myosin heavy chains are encoded by two genes located on different chromosomes. Circ. Res. 69 (2), 530–539.

Takeda, K., Yu, Z.X., Qian, S., Chin, T.K., Adelstein, R.S., Ferrans, V.J., 2000. Nonmuscle myosin II localizes to the Z-lines and intercalated discs of cardiac muscle and to the Z-lines of skeletal muscle. Cell Motil. Cytoskeleton 46 (1), 59–68.

Tullio, A.N., Accili, D., Ferrans, V.J., Yu, Z.X., Takeda, K., Grinberg, A., Westphal, H., Preston, Y.A., Adelstein, R.S., 1997. Nonmuscle myosin II-B is required for normal development of the mouse heart. Proc. Natl. Acad. Sci. U. S. A. 94 (23), 12407–12412.

Van Laer, L., Cryns, K., Smith, R.J., Van Camp, G., 2003. Nonsyndromic hearing loss. Ear Hear. 24 (4), 275–288.

Wright, R.B., Glantz, R.H., Butcher, J., 1988. Hearing loss in myotonic dystrophy. Ann. Neurol. 23 (2), 202–203.

Yang, T., Pfister, M., Blin, N., Zenner, H.P., Pusch, C.M., Smith, R.J., 2005. Genetic heterogeneity of deafness phenotypes linked to DFNA4. Am. J. Med. Genet. 139 (1), 9–12.

Zerylnick, C., Torroni, A., Sherman, S.L., Warren, S.T., 1995. Normal variation at the myotonic dystrophy locus in global human populations. Am. J. Hum. Genet. 56 (1), 123–130 Jan.